

Uncovering the dynamic precursors to motor-driven contraction of active gels

José Alvarado^{1,2,\$}, Luca Cipelletti^{3,*}, Gijsje H. Koenderink^{1,#,*}

¹ AMOLF, Living Matter Department, 1098 XG Amsterdam, Netherlands

² Massachusetts Institute of Technology, Department of Mechanical Engineering, Cambridge, MA, 02139, USA

³ L2C, Univ. Montpellier, CNRS, Montpellier, France

^{\$} Current address: University of Texas at Austin, Department of Physics, Austin, TX, 78712, USA

[#] Current address: Department of Bionanoscience, Kavli Institute of Nanoscience Delft, Delft University of Technology, 2629 HZ Delft, the Netherlands

^{*} Corresponding authors. LC: luca.cipelletti@umontpellier.fr; GK: g.h.koenderink@tudelft.nl

SUPPLEMENTAL MATERIAL

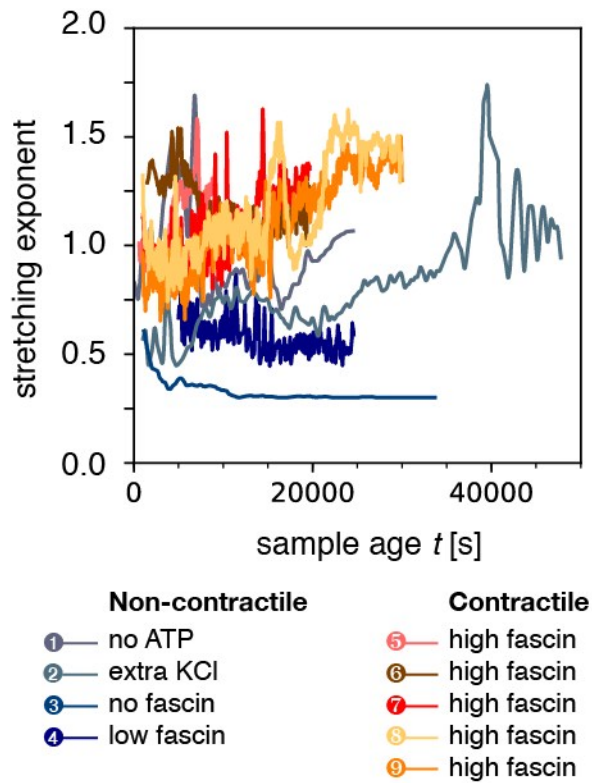


Figure S1. Temporal evolution of the stretching exponent β for all nine samples presented in this study (all with $q = 12.0 \mu\text{m}^{-1}$). The stretching exponent was obtained by fitting correlation functions averaged over a time bin of size $\Delta t = 50$ s for samples 1–3, and 10 s for samples 4–9. As a result, the data for samples 4–9 appear noisier.

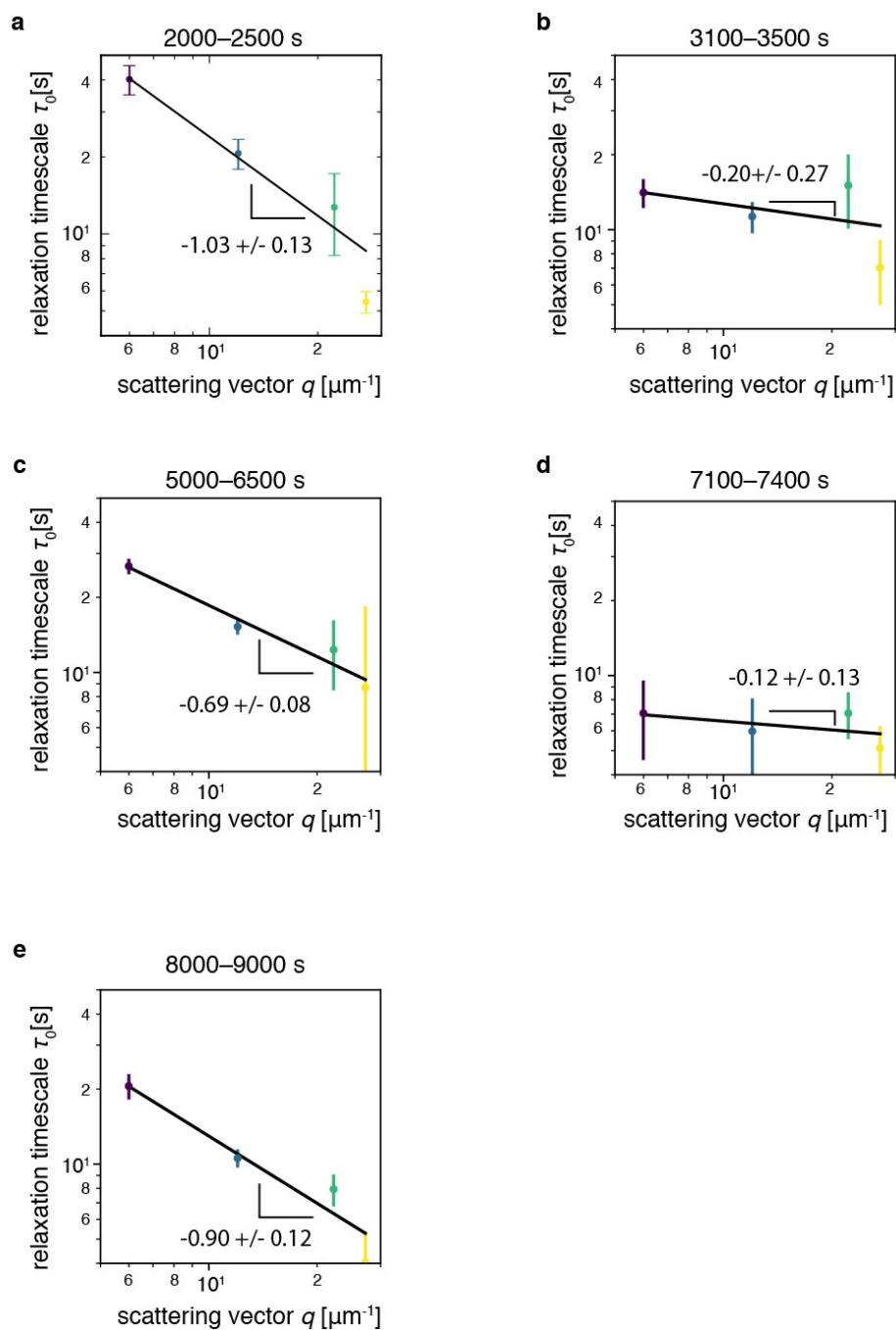


Figure S2. Plot of the relaxation timescale τ_0 of contractile sample 5 as a function of the scattering vector q over various sample age windows: (a) 2000–2500 s, (b) 3100–3500 s, (c) 5000–6500 s, (d) 7100–7400 s, and (e) 8000–9000 s.

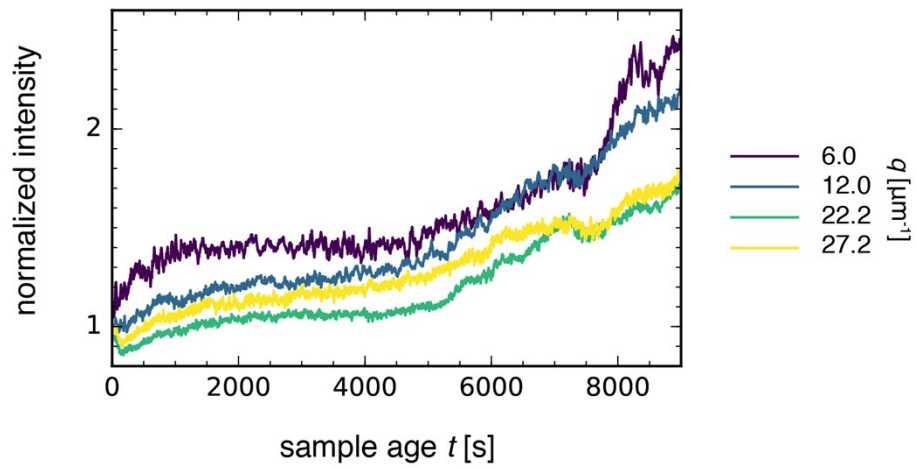


Figure S3. Normalized intensity I / I_0 of contractile sample 5 as a function of sample age t . The four curves correspond to different scattering vectors q (see legend, right).

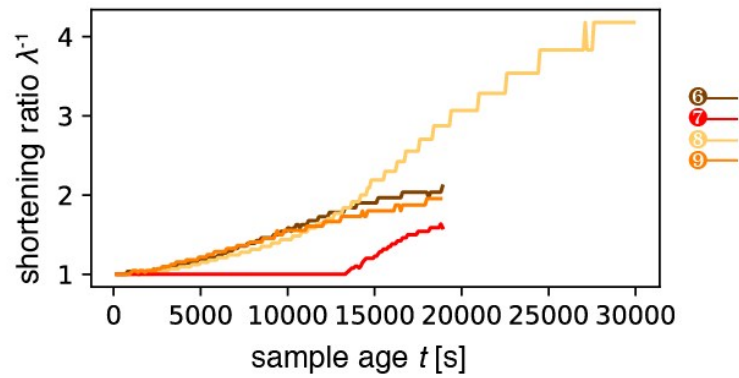


Figure S4. Contraction ratio λ^{-1} as a function of sample age t for contractile samples that have been measured simultaneously in real- and Fourier-space. The samples contain either 60 nM myosin (samples 7, 8, 9) or 120 nM myosin (sample 6). Curve colors correspond to sample number, see legend right.

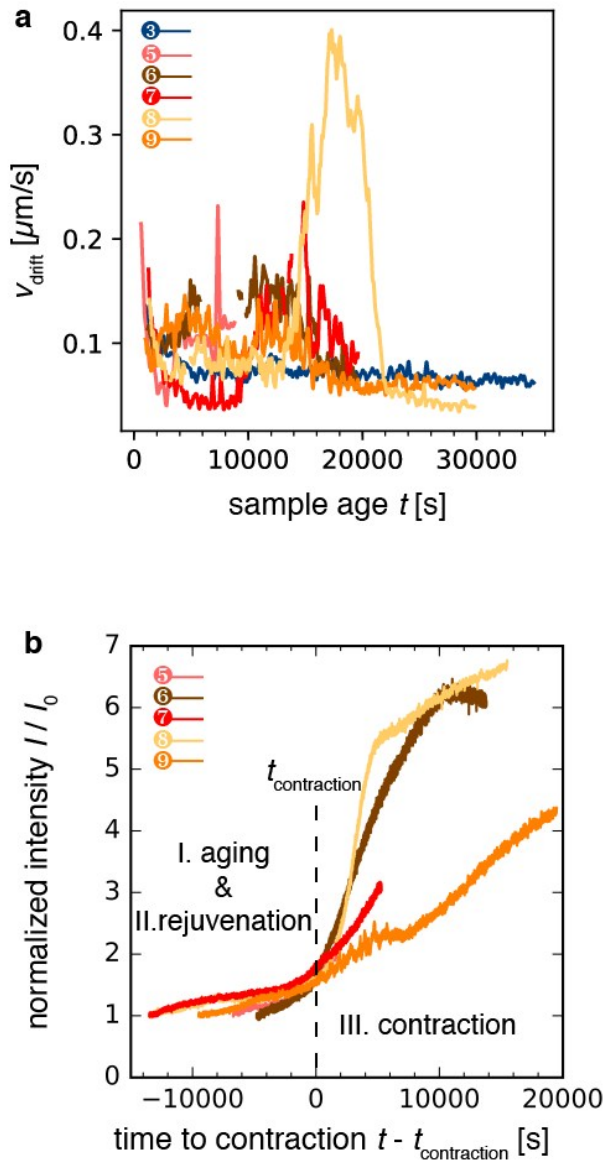


Figure S5. (a) Drift velocity v_{drift} of speckles in the imaging plane of the CCD as a function of sample age t , for all five active contractile gels, and for one active, but non-contractile sample (sample 3, $[\text{fascin}] = 0 \mu\text{M}$). (b) Average scattered intensity I normalized by the initial average intensity I_0 as a function of sample age t for all five contractile samples. Curve color corresponds to sample number, see legend left. The biochemical conditions are summarized in Table 1. The vertical dashed line indicates the onset of contraction as defined by the normalized intensity attaining a value of 1.5, which separates the stages of aging (I) and rejuvenation (II) from the contraction stage (III).

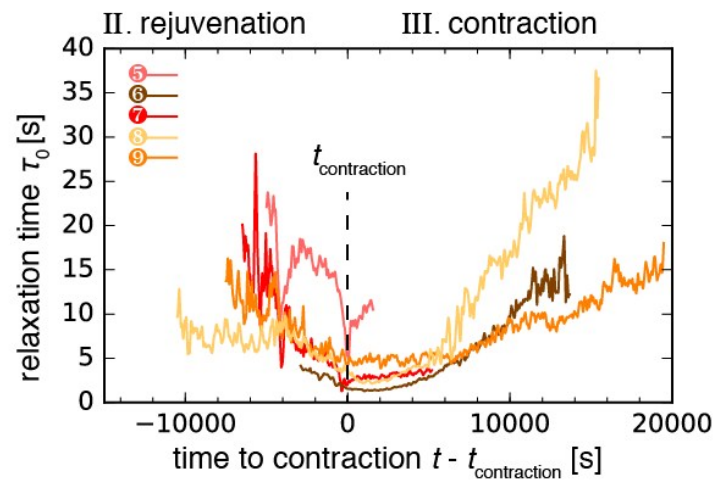


Figure S6. Relaxation time τ_0 as a function of time to contraction, $t - t_{\text{contraction}}$, for the rejuvenation and contraction stages. Dashed vertical line denotes $t_{\text{contraction}}$, which separates stage II from stage III. Note that the beginning of the rejuvenation stage can occur up to 10000 s before contraction. Curve color corresponds to sample number, see legend left and Table 1.

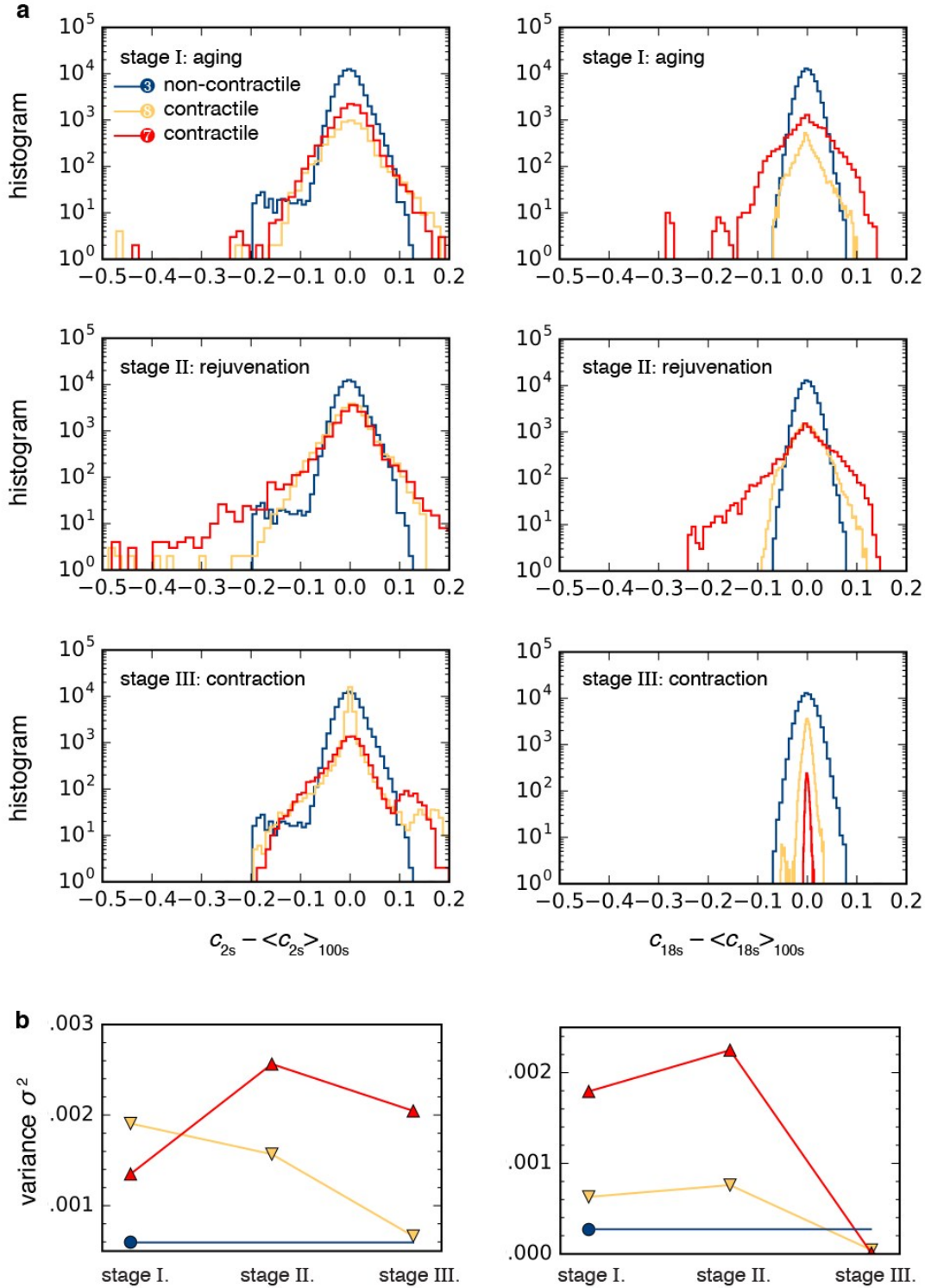


Figure S7. Statistics of the degree of correlation fluctuations $c_\tau - \langle c_\tau \rangle_{100s}$ for the three stages of sample evolution. (a) Histogram of $c_\tau - \langle c_\tau \rangle_{100s}$ for two different lag times, $\tau = 2s$ (left column) and $\tau = 18s$ (right column), broken down by stage. (Cf. main text, Fig. 7d, where $\tau = 6s$.) (b) Corresponding variance σ^2 for lag times $\tau = 2s$ (left) and $\tau = 8s$ (right). Color and symbol denote sample type: non-contractile sample 3 (blue, circle), contractile sample 8 (orange, downward triangles), and contractile sample 7 (red, upward triangles).

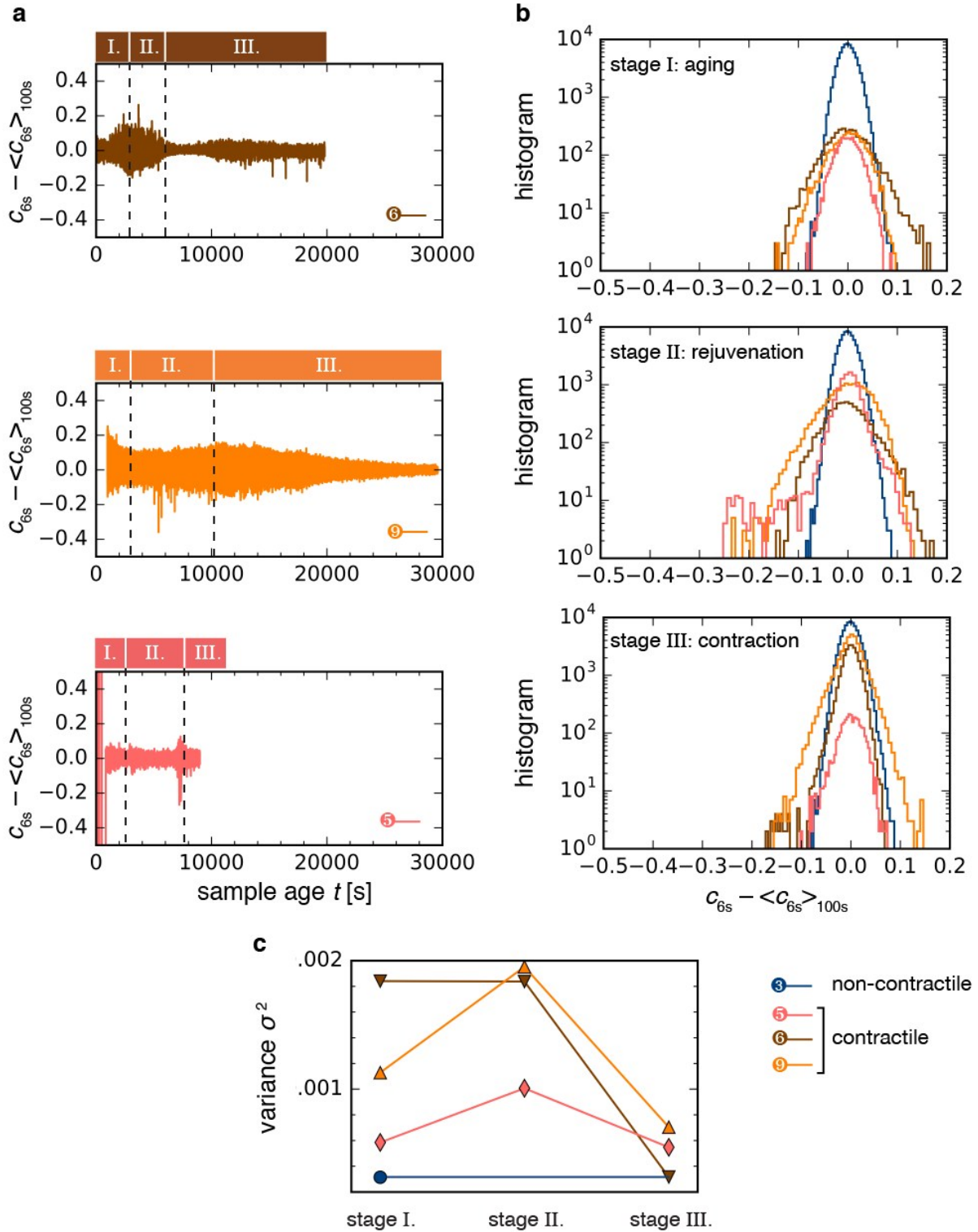
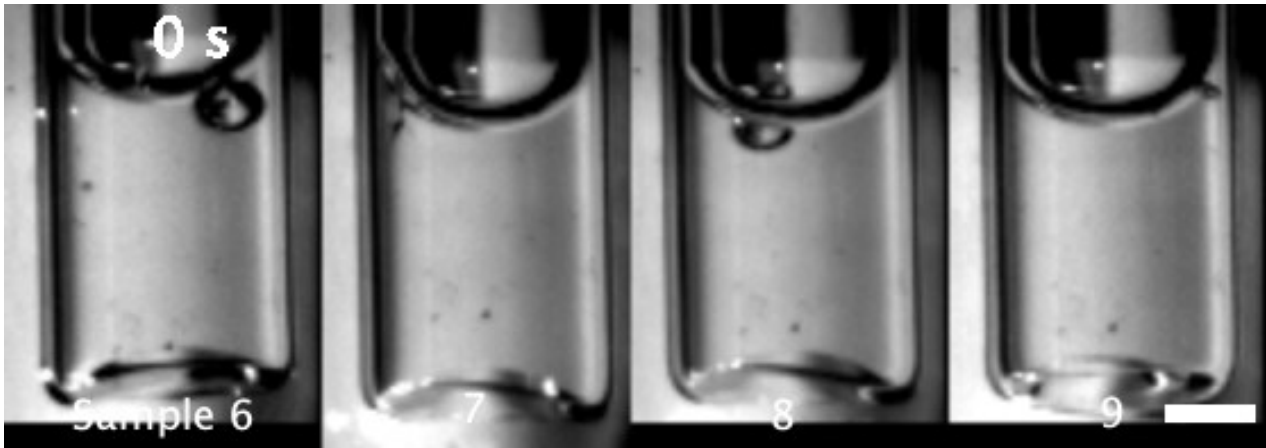
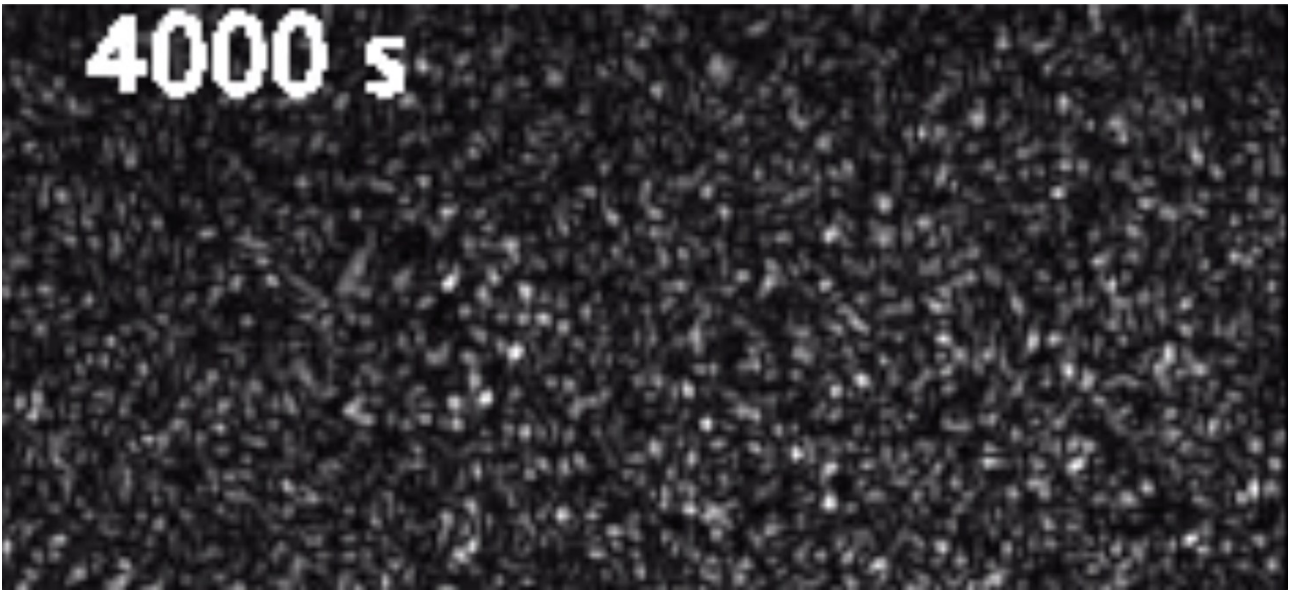


Figure S8. Statistics of samples not covered in the main text. The increased variance in stage II depicted in Fig. 7e also holds for these samples. (a) Degree of correlation, as in Fig. 7a–c. (b) Histograms for the three samples and the three stages shown in panel a. For reference, data of non-contractile sample 3 from Fig. 7 is also shown here (blue, circles). (c) Variance σ^2 of the distributions shown in panel b: contractile sample 6 (brown downward triangles), contractile sample 9 (orange, upward triangles), contractile sample 5 (pink, diamonds).



Movie 1. Real-space movies of the four contractile samples (6–9) which were imaged simultaneously in real and Fourier space. All samples have $[\text{fascin}] = 0.6 \mu\text{M}$, $[\text{actin}] = 12 \mu\text{M}$, $[\text{ATP}] = 0.1 \text{ mM}$. Sample 6 has $[\text{myosin}] = 0.12 \mu\text{M}$. Samples 7–9 have $[\text{myosin}] = 0.06 \mu\text{M}$. (left) Samples 6, 8, and 9 contract after a lag time of approximately 2000 s. Sample 7 contracts after a lag time of approximately 12000 s. Scale bar 2 mm. Sample age is given in the top-left corner.



Movie 2. This movie begins by depicting a typical speckle pattern corresponding to the scattering of laser light by the actin-myosin gel. At 6000 s, a bright, round, shimmering object can be seen rising as the sample contracts. This object very likely corresponds to a bubble. Bubbles scatter more strongly than the gel, and would therefore appear brighter in our imaging setup. We excluded samples exhibiting such evidence of bubbles from further analysis.